Laminin Compensation in Collagen α3(IV) Knockout (Alport) Glomeruli Contributes to Permeability Defects

Dale R. Abrahamson,* Kathryn Isom,* Eileen Roach,* Larysa Stroganova,* Adrian Zelenchuk,* Jeffrey H. Miner,† and Patricia L. St. John*

*Department of Anatomy and Cell Biology, University of Kansas Medical Center, Kansas City, Kansas; and †Renal Division, Department of Internal Medicine, Washington University, St. Louis, Missouri

ABSTRACT

Alport disease is caused by mutations in genes encoding the α3, α4, or α5 chains of type IV collagen, which form the collagenous network of mature glomerular basement membrane (GBM). In the absence of α3, α4, α5 (IV) collagen, α1, α2 (IV) collagen persists, which ordinarily is found only in GBM of developing kidney. In addition to dysregulation of collagen IV, Alport GBM contains aberrant laminins, which may contribute to the progressive GBM thickening and splitting, proteinuria, and renal failure seen in this disorder. This study sought to characterize further the laminin dysregulation in collagen α3(IV) knockout mice, a model of Alport disease. With the use of confocal microscopy, laminin α1 and α5 abundance was quantified, and it was found that they co-distributed in significantly large amounts in areas of GBM thickening. In addition, labeling of entire glomeruli for laminin α5 was significantly greater in Alport mice than in wild-type siblings. Reverse transcriptase–PCR from isolated glomeruli demonstrated significantly more laminin α5 mRNA in Alport mice than in wild-type controls, indicating upregulated transcription of *Lama5*. For testing glomerular barrier function, ferritin was injected into 2-wk-old Alport and control mice, and GBM was examined by electron microscopy. Highest ferritin levels were seen in Alport GBM thickenings beneath effaced podocyte foot processes, but morphologically normal GBM was significantly permeable as well. We concluded that (*1*) ultrastructurally normal Alport GBM residing beneath differentiated podocyte foot processes is inherently and abnormally permeable, and (*2*) upregulation of *Lama5* transcription and concentration of laminin α1 and α5 within Alport GBM thickenings contribute to abnormal permeabilities.

J Am Soc Nephrol 18: 2465–2472, 2007. doi: 10.1681/ASN.2007030328

Alport syndrome is caused by mutations in the *COL4A3*, *COL4A4*, or *COL4A5* genes, which encodes the type IV collagen α3, α4, and α5 chains, respectively, that compose the collagenous network within mature kidney glomerular basement membranes (GBM).[1–3] When any one of the *COL4A3* through *A5* genes is mutated, a stable α3, α4, α5 (IV) network cannot form, and immunolabeling techniques show an absence of these proteins in Alport GBM. In kidney, the disease is marked by hematuria of glomerular origin, thickening and splitting of the GBM, effacement of podocyte foot processes, progressive proteinuria, and declining renal function that usually requires replacement therapy.[1–3] Although several hundred mutations in human *COL4A3* through *A5* genes have been described in detail, exactly how these contribute to the glomerular pathogenesis of Alport disease remains unclear. Among other possibilities, a network of collagen α1, α2 (IV), which is present normally in developing GBM but removed during maturation,[4]

Received March 17, 2007. Accepted May 14, 2007.

Published online ahead of print. Publication date available at www.jasn.org.

Correspondence: Dr. Dale R. Abrahamson, Department of Anatomy and Cell Biology, University of Kansas Medical Center, MS 3038, 3901 Rainbow Boulevard, Kansas City, KS 66160. Phone: 913-588-7000; Fax: 913-588-2710; E-mail: dabrahamson@kumc.edu

has been shown to persist in Alport glomeruli, presumably because of an absence of collagen α3, α4, α5 (IV).[5] The α1, α2 (IV) network has different structural properties than α3, α4, α5 (IV) and may confer different behavioral signals to the adherent glomerular endothelial cells and podocytes as well. In addition, the α1, α2 (IV) network seems to be more susceptible to proteolysis, which over time could result in the GBM multilamination commonly seen in Alport kidneys.[5] Along these lines, recent studies have shown that human and mouse Alport glomeruli express unusually high amounts of a potent protease, macrophage metalloelastase (MMP-12), and treatment of Alport mice with a specific inhibitor of this enzyme improves GBM morphology and glomerular barrier function.[6]

In addition to the retention of collagen α1, α2 (IV) in Alport GBM, ectopic deposition of laminins has been documented in patients with Alport and in dog and mouse models of the disease.[7] Specifically, abnormal accumulations of laminin α1, α2, and β1 chains have been reported in Alport GBM,[7] whereas normal GBM contains only laminin $\alpha5\beta2\gamma1$ (LM-521) heterotrimers.[8] Previously, we showed in 4-wk-old Alport mice that both glomerular endothelial cells and podocytes are origins for laminin α1 and β1,[9] which normally are made by these cells only during the earliest stages of glomerular development.[10] Moreover, we localized these proteins by immunoelectron microscopy specifically to areas of GBM thickening that underlie effaced foot processes, suggesting that ectopic laminin deposition contributed to or possibly caused the GBM and podocyte deformations.[10] To examine the laminin dysregulation that takes place during the course of Alport disease more thoroughly, here we quantified laminin abundance within normal and Alport GBM using confocal microscopy and quantified laminin mRNA by reverse transcriptase–PCR (RT-PCR). In addition, to test the barrier properties of Alport GBM, we injected the ultrastructural tracer ferritin into normal and Alport mice and carried out electron microscopy. Our findings show that laminin α5 mRNA and protein were significantly upregulated in Alport glomeruli. In addition, Alport GBM was significantly more permeable to ferritin than wild-type GBM, particularly in areas of thickening and foot process effacement but also in areas that were ultrastructurally normal.

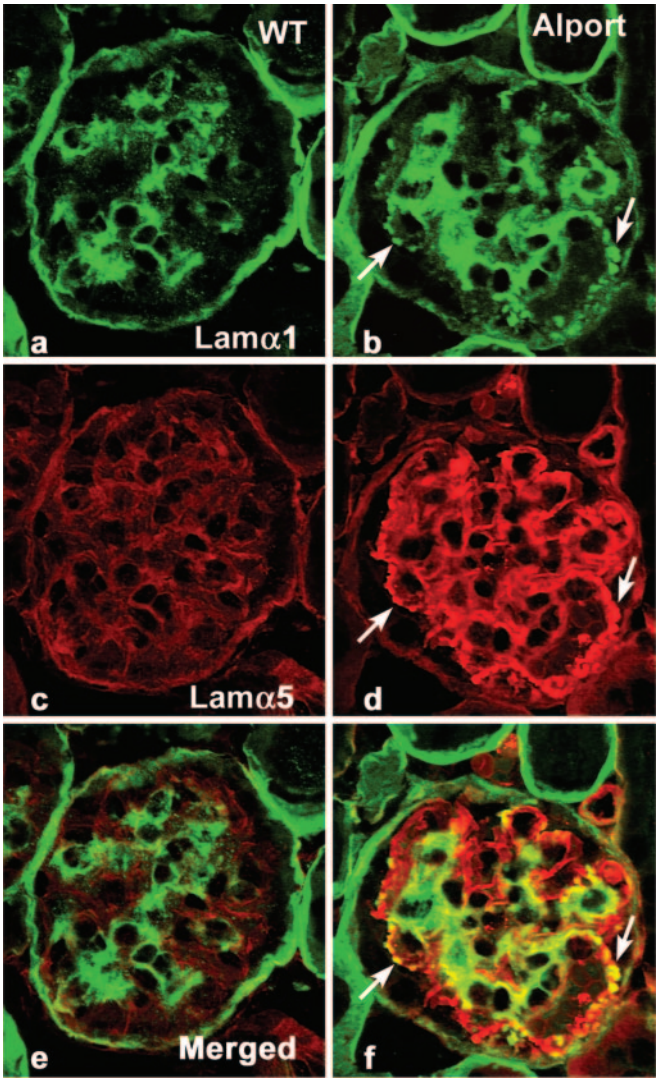

Figure 1. Immunofluorescence micrographs showing distribution of laminin α1 and α5 chains in wild-type (WT; a, c, and e) and Alport glomeruli (b, d, and f). Merged image (f) shows co-localization of laminin α1 and α5 chains to bright yellow nodules of peripheral capillary loop glomerular basement membranes (GBM) of Alport glomeruli (arrows). No co-localization is seen in wild-type glomeruli (e).

RESULTS

Quantification of GBM Laminin Dysregulation

When cryostat sections from 4-wk-old wild-type mouse kidneys were doubly immunolabeled for laminin α1 and α5 chains and viewed by confocal microscopy, the immunolabels rarely overlapped in glomeruli (Figure 1, a, c, and e). Laminin α1 chain (fluorescein) was concentrated within mesangial areas, whereas laminin α5 (rhodamine) localized specifically to peripheral loop GBM. By contrast, there was extensive label overlap in glomeruli from Alport littermates (Figure 1, b, d, and f), and many peripheral loop GBM contained yellow/orange nodules indicating co-localization of both laminin α1 and α5 chains to the same GBM sites (Figure 1f). In addition, the overall immunofluorescence intensities for laminin α5 appeared considerably brighter for Alport glomeruli (Figure 1d) when compared with controls (Figure 1c).

For quantification of total glomerular fluorescence intensities, red and green confocal images were each converted to grayscale, and examples for how images were masked and glomerular fluorescence signals collected are shown in Figure 2. Fluorescence pixel densities were measured only in areas included within the circular apertures. Despite the appearance of a somewhat brighter signal for laminin α1 in Alport glomeruli in selected images, no statistically significant differences were observed for total glomerular fluorescence intensities when

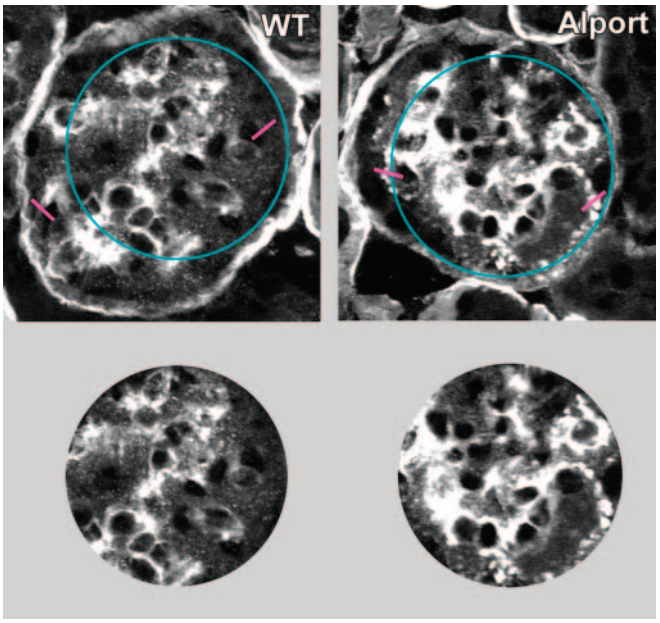

Figure 2. Grayscale images of Figure 1, a and b, showing positioning of measuring aperture (blue circle) and GBM bisecting tool (pink lines) used to quantify confocal immunofluorescence signal intensities.

compared with normal controls (Figure 3). Conversely, Alport glomeruli displayed an almost six-fold increase in total immunofluorescence intensity for laminin α5 chain (Figure 3).

To compare the relative abundance of laminin α chains within the GBM nodules characteristic of Alport glomeruli, we also quantified immunofluorescence intensities across specific, bisected GBM segments. This was also accomplished using Scion software that integrated fluorescence intensities across selected widths of glomerular capillaries (shown as bright pink bars in Figure 2). In these cases, Alport GBM segments contained approximately five-fold more immunolabel for laminin α1 and four-fold more label for laminin α5 than seen in bisected GBM from normal littermates (Figure 3).

Conceivably, the increased immunolabeling for laminin α5 seen throughout Alport GBM could have been due to (*1*) GBM disorganization and an accompanying increased epitope exposure to anti-α5 or (*2*) actual increases in laminin α5 protein deposition. To address the second possibility, we isolated glomeruli from 4-wk-old Alport and wild-type mice and analyzed glomerular mRNA by quantitative RT-PCR. Figure 4a shows a representative preparation obtained using the Dynabead isolation technique, which provides a fraction greatly enriched for glomeruli and with few tubular segments. Our quantitative RT-PCR results showed approximately 50% more laminin α5 mRNA in Alport glomeruli than in wild-type controls (Figure 4b). Taken together with the confocal quantification, our findings document increased biosynthesis of laminin α5 in Alport glomeruli, and we attribute this to a compensatory response to the absence of the collagen α3, α4, α5 (IV) network.

Abnormal Ferritin Permeability in Alport GBM

For examination of GBM permeability properties, ferritin was injected intravenously into 2-wk-old normal and Alport mice, and kidneys were fixed for electron microscopy 40 min after injection. As shown in Figure 5a, discrete ferritin particles were readily observed within GBM of normal mice. However, these were found predominantly within the subendothelial layer, and comparatively few ferritin particles penetrated the full width of the GBM to the level of the podocytes. For quantification of ferritin penetrability, GBM was digitally dissected free of adherent endothelial cells and podocytes, and ferritin particles were pseudocolored (Figure 5b). GBM were then further dissected into their separate subendothelial and subepithelial halves (Figure 5c), and the numbers of ferritin particles within each layer were then scored. In all, 1326 ferritin particles were seen throughout 125 linear μm of GBM of wild-type/heterozygous mice. Our results showed that the outer subepithelial half of wild-type GBM contained approximately one

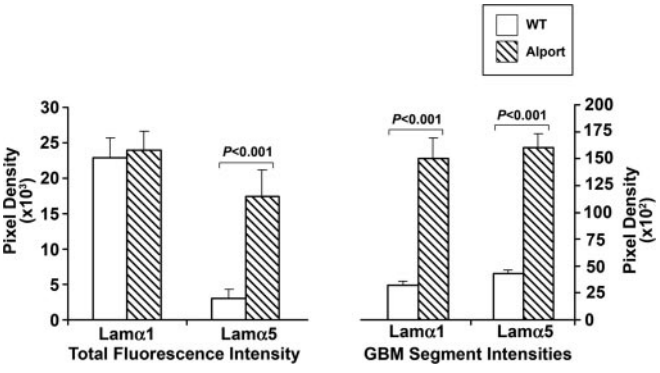

Figure 3. Histograms showing confocal immunofluorescence intensities for laminin α1 and α5 chains in WT and Alport glomeruli. Highly significant increases were seen for laminin α5 in sections through whole glomeruli and for both laminin α1 and α5 across segments of GBM. n = 17 glomeruli for WT and 18 for Alport; 18 GBM segment intensities for both genotypes.

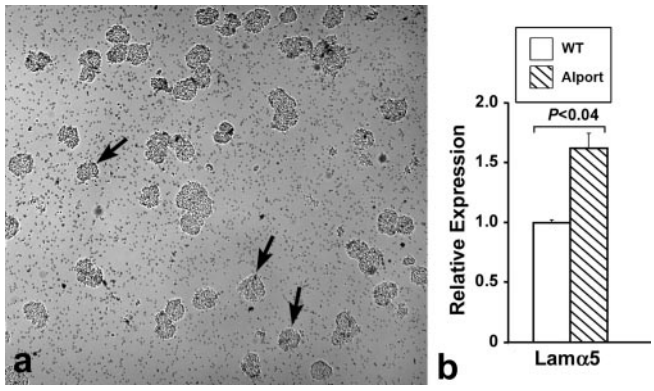

Figure 4. (a) Whole-mount view of representative preparation of isolated glomeruli (arrows). Small dots are magnetic beads. (b) Quantitative reverse transcriptase–PCR analysis, showing significant upregulation of laminin α5 mRNA in Alport glomeruli (n = 3 WT and 3 Alport samples).

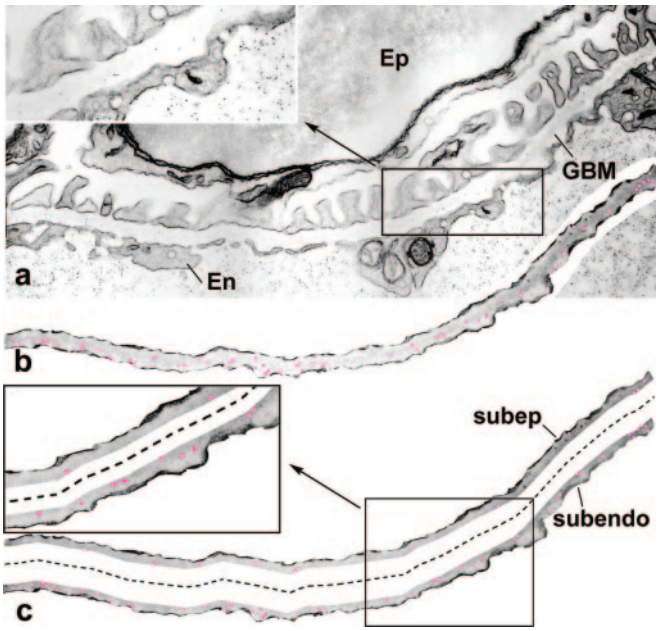

Figure 5. Electron micrographs of glomerular capillary wall (a) from 2-wk-old mouse that received an intravenous injection of ferritin. Insert in A shows ferritin (small electron-dense dots) within the GBM. (b) The same length of GBM shown in A digitally microdissected and with ferritin particles pseudocolored pink. (c) GBM further microdissected into subendothelial (subendo) and subepithelial (subep) halves. Insert in (c) shows that relatively few ferritin particles penetrate the subepithelial layer of WT GBM.

third the number of particles found within the inner, subendothelial half (Figures 5 and 6).

Undertaking the same approach with Alport mice showed more ferritin within the GBM overall (2418 particles were found in 127 linear μm of GBM) and within the subepithelial half in particular (Figures 6 and 7). This was borne out by

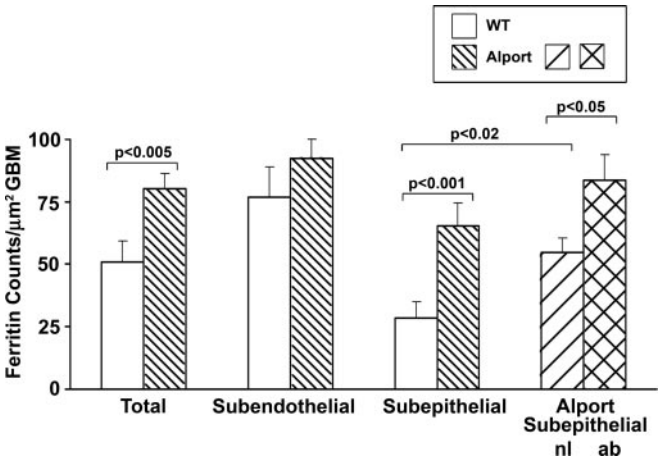

Figure 6. Histogram showing numbers of ferritin particles/μm^2 GBM in 2-wk-old WT and Alport mice. In Alport mice, significantly more ferritin permeated the total width of GBM, subepithelial halves, and subepithelial segments with normal (nl) GBM and podocyte architecture as well as abnormal (ab) segments.

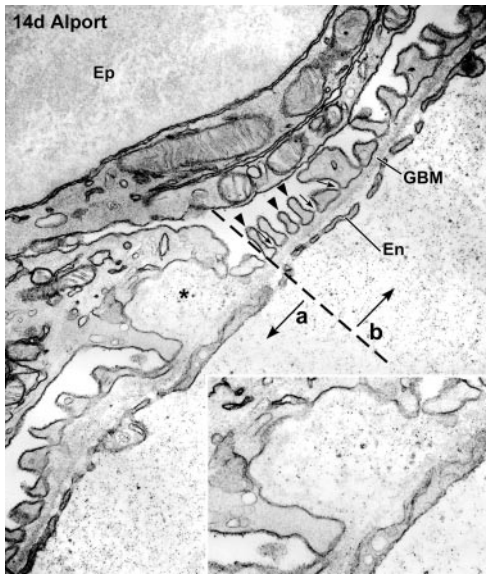

Figure 7. Glomerular capillary wall from 2-wk-old Alport mice that received ferritin intravenously. Ferritin can be visualized throughout the GBM, including areas of subepithelial projections (*) beneath effaced foot processes. Insert shows higher magnification view of (*). Region to the left of segment marked (a) illustrates abnormal GBM and podocyte architecture, whereas region to the right marked (b) contains normal GBM morphology, podocyte foot process registration (arrowheads), and epithelial slit diaphragms (arrows).

statistical comparisons of ferritin counts between Alport and normal GBM, which revealed that significantly more ferritin was found within Alport GBM, especially subepithelial layers (Figure 6). Average ferritin/μm^2 within subendothelial layers was also somewhat higher in Alport than normal GBM, but this apparent difference was not statistically significant (Figure 6).

Glomerular capillary walls in 2-wk-old Alport mice contained large areas that appear morphologically normal. Specifically, GBM architecture, podocyte foot process registration, and slit diaphragm formation all were indistinguishable from those of wild-type mice (Figure 7). Intermingled with these normal areas were smaller regions containing pronounced GBM deformations and podocyte abnormalities (Figure 7). We therefore evaluated ferritin penetrability in morphologically normal and abnormal zones of these 2-wk-old Alport glomeruli (Figures 7 and 8). This analysis showed that the outer, subepithelial half within morphologically normal areas of Alport glomeruli was significantly more permeable to ferritin than in wild-type controls (Figure 6). However, maximal permeabilities occurred in the morphologically abnormal regions containing subepithelial GBM humps and foot process effacement (Figures 6 through 8).

In addition to greatly increased penetration of ferritin into 2-wk-old Alport GBM, ferritin was detected in intracellular vesicles within podocytes (Figure 9). At 4 and 6 wk of age, Alport glomeruli progressively became more severely dam-

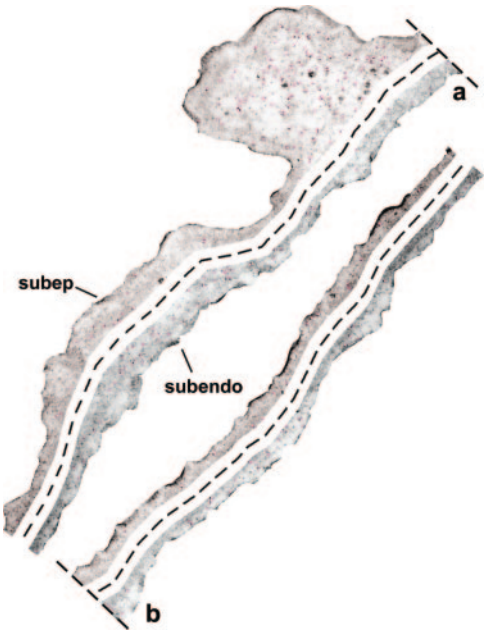

Figure 8. Microdissected GBM from regions (a) and (b) from Figure 7, with ferritin pseudocolored pink.

aged, GBM was greatly thickened and often multilaminated, and podocytes accumulated large amounts of ferritin within intracellular vesicles and lysosomes (Figure 10). Ferritin was also readily detected within apical intracellular vesicles of proximal tubule epithelial cells (Figure 11). Ferritin was never detected intracellularly within podocytes or tubular epithelial cells in 2- or 4-wk-old heterozygous or wild-type kidneys.

DISCUSSION

Earlier studies that were conducted in Alport patients, as well as in dog and mouse models of the disease, showed laminin dysregulation in GBM of all three species.[7] Our previous findings in mice showed that laminin α1 chain, which is normally restricted to the mesangium in maturing glomeruli, also immunolocalizes specifically to the peripheral loop irregularities characteristic of Alport GBM.[9] Here, we sought to quantify the magnitude of laminin expression in Alport mouse glomeruli.

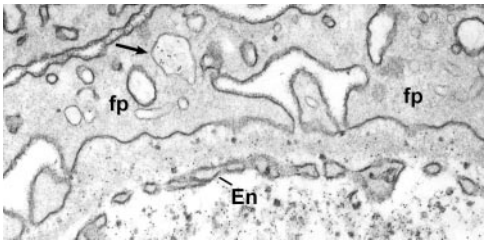

Figure 9. Glomerular capillary wall from 2-wk-old Alport mouse. Ferritin fully penetrates the GBM and is also seen in intracellular vesicles within podocytes (arrow). Note unusually broad foot processes (fp). En, endothelium.

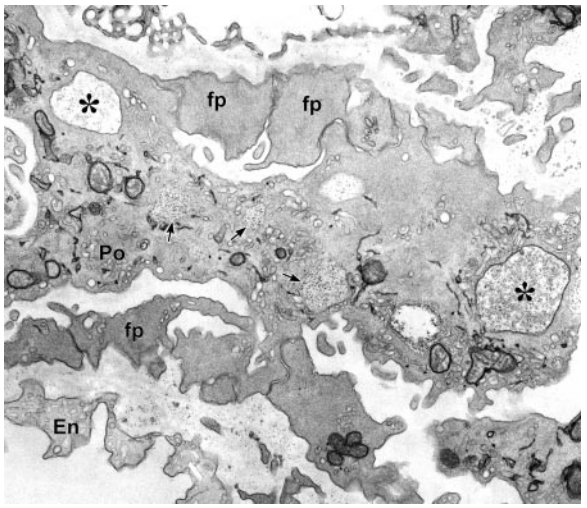

Figure 10. Glomerulus from 6-wk-old Alport mouse. Podocytes (Po) are severely damaged, and only broadly effaced foot processes (fp) are seen at this age. Numerous ferritin particles are present within intracellular vesicles (*) and lysosomes (arrows).

Our quantitative immunofluorescence results showed no differences in overall glomerular labeling for laminin α1, but significantly more laminin α1 immunolocalized to discrete areas of GBM thickening in capillary loops. In addition, considerably more immunolabeling for laminin α5 was found throughout Alport glomeruli than in wild-type, and especially in the GBM irregularities where laminin α1 was abnormally deposited as well. Quantitative PCR similarly showed an upregulation of laminin α5 mRNA, indicating that the increased total

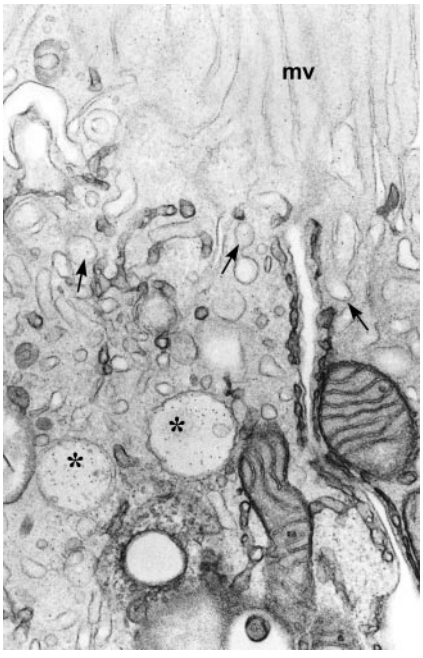

Figure 11. Apical region of proximal convoluted tubule epithelium from 6-wk-old Alport mouse. Ferritin is seen in apical endocytic vesicles (arrows) at the bases of microvilli (mv), as well as within lysosomes (*).

glomerular immunofluorescence was most likely a consequence of activation of *Lama5* gene transcription. We also carried out electron microscopic studies using the ultrastructural tracer ferritin to compare regional permeability properties of the developing glomerular capillary wall in Alport mice and normal littermates. Our ferritin injection results showed that the Alport GBM was abnormally permeable and that maximal permeabilities occurred specifically in capillary wall segments containing GBM thickenings and effaced foot processes of podocytes. Nevertheless, significant ferritin permeabilities were also observed in Alport mice in areas where GBM and podocyte foot process ultrastructure appeared entirely normal, signifying that the Alport GBM was inherently defective in its barrier properties. Taken together with the loss of the collagen α3, α4, α5 (IV) network, our findings indicate that dysregulation of laminin synthesis and distribution in Alport glomeruli lead to the striking structural and functional deficits seen in this disorder.

Mechanisms regulating the synthesis of different laminins and governing their microanatomic distribution patterns are poorly understood. Nevertheless, the appearance and disappearance of various laminin isoforms in GBM of developing glomeruli have been well described.[8] First, basement membranes in the vascular cleft region of comma- and S-shaped nephrons contain LM-111 and -411. As glomeruli progress into the capillary loop stage, these isoforms are quickly eliminated and replaced by LM-521, which becomes the only laminin present in the GBM of maturing stage glomeruli and thereafter. Immunoelectron microscopic localization experiments have shown that both glomerular endothelial cells and podocytes synthesize LM-111 and -521 at the appropriate stages of development, but events regulating the isoform switches at the gene and protein level are unknown.[10]

Our previous immunofluorescence evidence showed that the disappearance of LM-111 occurs normally in early glomeruli of Alport kidneys.[9] However, LM-111 reappears during early capillary loop stages, and immunoelectron microscopy documented that synthesis resumes in both glomerular endothelial cells and podocytes at this stage. Although our findings presented here showed no differences in total glomerular immunofluorescence intensities for laminin α1, there were marked increases in laminin α1 immunolabeling in the irregular GBM thickenings that typify Alport glomeruli, particularly where immunolabeling also indicated unusually large amounts of laminin α5. In addition, there were significant increases in total glomerular immunolabeling for laminin α5, and quantitative RT-PCR experiments showed marked increases in laminin α5 mRNA in Alport glomeruli as well. This increased tempo in laminin α5 synthesis may therefore represent a cellular response to the absence of the collagen α3, α4, α5 (IV) network that typifies the Alport GBM.

Although exactly how the Alport condition affects glomerular laminin gene transcription is not known, likely mediators probably involve cell–matrix adhesion receptors, especially the integrins. The most abundant integrins expressed within the glomerulus include the $\alpha1\beta1$, $\alpha2\beta1$, and $\alpha3\beta1$ heterodimers, and they each immunolocalize to restricted compartments: $\alpha1\beta1$ integrin is found chiefly on mesangial cells, $\alpha2\beta1$ occurs largely on endothelial cells, and $\alpha3\beta1$ is highly expressed on basal membranes of podocytes.[12] Specifically how these proteins direct glomerular cell behaviors and alter gene transcription patterns *in vivo* remains incompletely defined, but studies with knockout mice have been informative. For example, when compared with Alport mice alone, double-knockout mice null at both the collagen α3 (IV) (Alport mice) and integrin α1 alleles have delayed onset and slower progression of disease, improved glomerular morphology, and a reduction of GBM laminin α2 and β1, which are also abnormally expressed in Alport GBM.[12] Because $\alpha1\beta1$ integrin is believed to be expressed chiefly if not exclusively by mesangial cells, how these proteins affect biosynthetic pathways in capillary endothelial cells and podocytes is unclear. Perhaps paracrine signaling from the mesangium somehow mediates matrix gene expression in endothelial cells and/or podocytes, as suggested previously.[12] However, mesangial cells are embedded in a matrix rich in collagen α1, α2 (IV) and generally not in direct contact with the GBM *per se*, so how an absence of α3, α4, α5 (IV) in GBM might initiate mesangial cell signaling is mysterious. Another candidate is $\alpha3\beta1$ integrin, which is a proven adhesion receptor for laminins and type IV collagen and located in the basal plasma membrane of podocytes.[11,13] When integrin α3 is deleted in mice, glomerular capillary branching is decreased, and this is accompanied by widespread disorganization and fragmentation of the GBM and a failure of podocyte foot process formation.[13] Although these changes were originally thought to be due mainly to a loss of cell–matrix adhesion in mutant podocytes, other studies have now shown that $\alpha3\beta1$ integrin can also associate with the tetraspanin CD151 cell–cell adhesion complex that, among other things, can indirectly regulate gene transcription as well.[14] Clearly, much additional work is required to understand ways in which aberrant GBM assembly can affect glomerular cell behavior, including transcription. Among other things, perhaps future studies that carefully inventory the abundance and distribution of the various integrins in Alport glomeruli will be useful. In addition, experiments that specifically examine transcriptional regulation of the laminin genes may shed light on mechanisms leading to glomerular fibrotic disorders, including Alport disease.

To evaluate permeability properties of the Alport GBM, we injected ferritin into mice, which is an approximately 480-kD protein complex and the main intracellular iron storage protein, making it useful as a quantifiable, electron-dense ultrastructural tracer. Although ferritin has been used as a glomerular permeability probe in a number of studies carried out in rats,[15,16] it has been used infrequently in mice. Recently, however, GBM of 1.5- to 2-wk-old laminin β2 null mice were shown to be abnormally permeable to ferritin, even in areas where foot process and epithelial slit diaphragm morphology seem intact.[17] When we injected ferritin into 2-wk-old wild-type mice, ferritin was readily distinguished within the GBM, although most of it was restricted to the inner, subendothelial

half. Nevertheless, quantities of ferritin fully penetrated the GBM up to the base of podocyte foot processes, probably reflecting an incompletely mature filtration barrier in mice at this age. In contrast, when injected into 2-wk-old Alport littermates, significantly more ferritin permeated the full width of the GBM than in wild-types. Maximal permeabilities were seen in areas of GBM thickening beneath abnormally broad foot processes, which are exactly the same sites where unusually large amounts of laminin α1 and α5 were deposited, indicating that the aberrantly distributed laminin contributed to the permeability defect. Importantly, significantly more ferritin also penetrated the subepithelial half of Alport GBM in areas where GBM architecture and foot process registration appeared entirely normal. These results therefore indicate that the Alport mouse GBM, like that of laminin β2 mutant mice, is inherently and abnormally permeable to circulating macromolecules, and these defects are apparently not due to errors in podocyte foot process formation and/or slit diaphragm integrity.

In addition to the GBM, our ferritin injection studies resulted in abundant localization of tracer intracellularly within vesicles and lysosomes of Alport podocytes and within intracellular vesicles in the apical cytoplasm of proximal tubule epithelial cells. Whether ferritin observed in the tubular epithelium breached the Alport glomerular filtration barrier by transcytosis through podocytes or by extracellular passage through filtration slit pores is unclear, and we are exploring both possibilities.

CONCISE METHODS

Animals

Mice that genetically lacked the α3(IV) collagen chain (Alport mice)[18] were purchased from Jackson Laboratory (Jax mouse strain 129-Col4a3^{tm1Dec}; Bar Harbor, ME). We maintained our colony by interbreeding heterozygotes, and genotyping was carried out by PCR. Heterozygous and wild-type littermates served as controls. All procedures with animals were approved by the Institutional Animal Care and Use Committee to ensure compliance with the Health Research Extension Act, Animal Welfare Act, and the Public Health Service Policy on Humane Care and Use of Laboratory Animals.

Confocal Microscopy and Image Analysis

Deeply anesthetized Alport and control littermate mice underwent nephrectomies at 4 wk of age, and kidneys were snap-frozen in isopentane chilled in dry ice–acetone bath. Cryostat sections, approximately 10 μm thick, were fixed for 10 min in 100% methanol and immunolabeled with chain-specific rat anti-mouse laminin α1 and rabbit anti-laminin α5 chain antibodies that were prepared and characterized as described previously.[19–21] Fluorescein- and rhodamine-conjugated secondary antibodies were obtained from ICN Biomedicals (Costa Mesa, CA). All slides that underwent confocal fluorescence quantification were immunolabeled with the same mixtures of antibodies on the same day and coverslipped overnight with ProLong anti-fade mounting media (Molecular Probes-Invitrogen, Carlsbad, CA). Slides were then viewed on a Zeiss LSM-510 scanning laser confocal microscope (Thornwood, NY), and Z-series images were captured at 0.2-μm intervals. All images were captured on the same day using constant laser intensity, confocal apertures, gain, and black-level parameters. Raw confocal images taken from the mid-regions of glomeruli on green (immunofluorescence for laminin α1 chain) and red channels (laminin α5 chain) were imported into Adobe Photoshop (San Jose, CA) and converted to grayscale, and output levels were set to a range of 0 to 250. Images were masked digitally with an opaque frame containing a fixed circular aperture with a diameter measuring 60 μm (slightly smaller than a mature glomerulus of a 2-wk-old mouse). Glomerular fields that did not fully occupy and extend beyond the aperture margins were not analyzed. Total pixel densities within only the unmasked (glomerular) areas were then measured with Scion software (http://www.scioncorp.com) as a relative measure for glomerular immunofluorescence intensities. Mean intensities were statistically compared using a *t* test. In addition, Scion software was used to bisect selected GBM segments, and fluorescence intensities across these segments were measured and compared statistically.

Glomerular Isolation and Real-Time PCR

Glomeruli were isolated from three 4-wk-old Alport and three wild-type mice (six separate glomerular preparations) using the magnetic bead method.[22] Briefly, mice were anesthetized with 1 mg/10 g body wt ketamine and 0.15 mg/10 g body wt xylazine. Blood was washed from the mice by cardiac perfusion with HBSS followed by perfusion of magnetic beads (Dynabead M-450, Invitrogen; 2×10^6 beads/ml in HBSS). Kidneys were removed and minced on ice, followed by digestion at 37°C with 1 mg/ml collagenase and 100 U/ml DNAse I for 30 min. Digested kidneys were filtered twice with 100 μ Falcon cell strainers, and tissue was pelleted by gentle centrifugation ($200 \times g$, 5 min). Glomeruli containing Dynabeads were collected using a magnetic particle concentrator (Dynal, Oslo, Norway), washed, and resuspended in HBSS three times. The final glomerular enriched fraction was pelleted, frozen immediately in liquid nitrogen, and stored at −80°C.

Total RNA was isolated from glomeruli using the RNAqueous-Micro spin kit (Ambion, Austin, TX). Samples were diluted to 10 ng/ml and amplified using QuantiTect SYBR Green RT-PCR kit (Qiagen, Valencia, CA) with the following primers: Laminin α5 forward 5′-ACC CAA GGA CCC ACC TGT AG-3′ and reverse 5′-TCA TGT GTG CGT AGC CTC TC-3′[23] and cyclophilin forward 5′-CAG ACG CCA CTG TCG CTT T-3′ and reverse 5′-TGT CTT TGG AAC TTT GTC TGC AA-3′.[24] Real-time PCR was performed using an iCycler (Bio-Rad, Hercules, CA). The primer sets were validated for efficiency by the comparative Ct method using standard curve analysis.[25] PCR products were analyzed on agarose gels to confirm size, and melt curve analysis was performed to reveal a single amplified product. RT-PCR product for cyclophilin was verified by sequencing using the KUMC Biotechnology Support Facility.

Ferritin Permeabilities

Horse spleen ferritin (32 mg/ml in 0.15 M NaCl) was injected intravenously through the saphenous vein into 2-wk-old (100 μl/mouse; three Alport, one heterozygous, two wild-type), 4-wk-old (150 μl;

two Alport, two wild-type), and 6-wk-old (200 μl; two Alport) anesthetized mice. Forty minutes after injection, kidneys were fixed *in situ* by clamping the hilus and simultaneously injecting Karnovsky fixative into the cortex. After 5 min, kidneys were removed, and cortices sliced into 1-mm cubes and fixed for an additional 90 min on ice. Tissue was then postfixed in ferrocyanide-reduced osmium[26] and routinely embedded in Polybed 812. Ultrathin sections were stained with 1:50 bismuth subnitrate for 5 min,[27] and multiple glomerular capillary loops from a minimum of 11 separate glomeruli (from two wild-type mice) and 12 separate glomeruli (from two Alport mice) were examined. Electron micrographic prints of cross-sectional planes through capillary walls were scanned into Photoshop; tangential sections were not evaluated further. Ferritin particles on the scans, recognized as discrete electron-dense spots, were pseudocolored, and lengths of GBM were dissected digitally into subendothelial and subepithelial halves. The numbers of ferritin particles/μm^2 within the separate subendothelial and subepithelial GBM layers were then counted using Scion software, and averages were compared statistically.

ACKNOWLEDGMENTS

Funds came from National Institutes of Health grants DK052483 and DK065123. Confocal images were acquired at the KUMC Confocal Imaging Facility, supported in part by the Kansas IDeA Network of Biomedical Research Excellence (RR016475).

Portions of this work were presented previously in abstract form (*J Am Soc Nephrol* 15: 418A, 2004 and *Matrix Biol* 25: S84–S85, 2006).

We thank Dr. Elizabeth Petroske for technical assistance.

DISCLOSURES

None.

REFERENCES

1. Hudson BG, Tryggvason K, Sundaramoorthy M, Neilson EG: Alport syndrome, Goodpasture syndrome, and type IV collagen. *N Engl J Med* 348: 2543–2556, 2003
2. Kashtan CE: Familial hematuria due to type IV collagen mutations: Alport syndrome and thin basement membrane nephropathy. *Curr Opin Pediatr* 16: 177–181, 2004
3. Kashtan CE: Familial hematurias: What we know and what we don't. *Pediatr Nephrol* 20: 1027–1035, 2005
4. Miner JH, Sanes JR: Collagen IV alpha 3, alpha 4, and alpha 5 chains in rodent basal laminae: Sequence, distribution, association with laminins, and developmental switches. *J Cell Biol* 127: 879–891, 1994
5. Kalluri R, Shield CF, Todd P, Hudson BG, Neilson EG: Isoform switching of type IV collagen is developmentally arrested in X-linked Alport syndrome leading to increased susceptibility of renal basement membranes to endoproteolysis. *J Clin Invest* 99: 2470–2478, 1997
6. Rao VH, Meehan DT, Delimont D, Nakajima M, Wada T, Gratton MA, Cosgrove D: Role for macrophage metalloelastase in glomerular basement membrane damage associated with Alport syndrome. *Am J Pathol* 169: 32–46, 2006
7. Kashtan CE, Kim Y, Lees GE, Thorner PS, Virtanen I, Miner JH: Abnormal glomerular basement membrane laminins in murine, canine, and human Alport syndrome: Aberrant laminin alpha 2 deposition is species independent. *J Am Soc Nephrol* 12: 252–260, 2001
8. Miner JH: Building the glomerulus: A matricentric view. *J Am Soc Nephrol* 16: 857–861, 2005
9. Abrahamson DR, Prettyman AC, Robert B, St. John PL: Laminin-1 reexpression in Alport mouse glomerular basement membranes. *Kidney Int* 63: 826–834, 2003
10. St. John PL, Abrahamson DR: Glomerular endothelial cells and podocytes jointly synthesize laminin-1 and -11 chains. *Kidney Int* 60: 1037–1046, 2001
11. Kreidberg JA, Symons JM: Integrins in kidney development, function, and disease. *Am J Physiol Renal Physiol* 279: F233–F242, 2000
12. Cosgrove D, Rodgers K, Meehan D, Mikker C, Bovard K, Gilroy A, Garner H, Kotelianski V, Gotwals P, Amatucci A, Kalluri R: Integrin alpha1beta1 and transforming growth factor-beta1 play distinct roles in Alport glomerular pathogenesis and serve as dual targets for metabolic therapy. *Am J Pathol* 157: 1649–1659, 2000
13. Kreidberg JA, Donovan MJ, Goldstein SL, Rennke H, Shepherd K, Jones RC, Jaenisch R: Alpha 3 beta 1 integrin has a crucial role in kidney and lung morphogenesis. *Development* 122: 3537–3547, 1996
14. Chattopadhyay N, Wang Z, Ashman LK, Brady-Kalnay SM, Kreidberg JA: alpha3beta1 integrin-CD151, a component of the cadherin-catenin complex, regulates PTPmu expression and cell-cell adhesion. *J Cell Biol* 163: 1351–1362, 2003
15. Farquhar MG, Wissig SL, Palade GE: Glomerular permeability I: Ferritin transfer across the normal glomerular capillary wall. *J Exp Med* 113: 47–66, 1961
16. Farquhar MG, Palade GE: Glomerular permeability II. Ferritin transfer across the glomerular capillary wall in nephrotic rats. *J Exp Med* 114: 699–716, 1961
17. Jarad G, Cunningham J, Shaw AS, Miner JH: Proteinuria precedes podocyte abnormalities in *Lamb2−/−* mice, implicating the glomerular basement membrane as an albumin barrier. *J Clin Invest* 116: 2272–2279, 2006
18. Cosgrove D, Meehan DT, Grunkemeyer JA, Kornak JM, Sayers R, Hunter WJ, Samuelson GC: Collagen COL4A3 knockout: A mouse model of Alport syndrome. *Genes Dev* 10: 1403–1413, 1996
19. Abrahamson DR, Irwin MH, St. John PL, Perry EW, Accavitti MA, Heck LW, Couchman JR: Selective immunoreactivities of kidney basement membranes to monoclonal antibodies against laminin: Localization of the end of the long arm and the short arms to discrete microdomains. *J Cell Biol* 109: 3477–3491, 1989
20. Miner JH, Patton BL, Lentz SI, Gilbert DJ, Snider WD, Jenkins NA, Copeland NG, Sanes JR: The laminin alpha chains: Expression, developmental transitions, and chromosomal locations of 1–5, identification of heterotrimeric laminins 8–11, and cloning of a novel 3 isoform. *J Cell Biol* 137: 685–701, 1997
21. St. John PL, Wang R, Yin Y, Miner JH, Robert B, Abrahamson DR: Glomerular laminin isoform transitions: Errors in metanephric culture corrected by grafting. *Am J Physiol* 280: F695–F705, 2001
22. Takemoto M, Asker N, Gerhardt H, Lundkvist A, Johansson BR, Saito Y, Betsholtz C: A new method for large scale isolation of kidney glomeruli from mice. *Am J Pathol* 161: 799–805, 2002
23. Shannon MB, Patton BL, Harvey SJ, Miner JH: A hypomorphic mutation in the mouse laminin alpha5 gene causes polycystic kidney disease. *J Am Soc Nephrol* 17: 1913–1922, 2006
24. Shih SC, Robinson GS, Perruzzi CA, Calvo A, Desai K, Green JE, Ali IU, Smith LE, Senger DR: Molecular profiling of angiogenesis markers. *Am J Pathol* 161: 35–41, 2002
25. Livak KJ, Schmittgen TD: Analysis of relative gene expression data using real-time quantitative PCR and the 2(-Delta Delta C(T)) method. *Methods* 25: 402–408, 2001
26. Karnovsky MJ: Use of ferrocyanide-reduced osmium tetroxide in electron microscopy [Abstract]. *Am Soc Cell Biol* 1971, p 146
27. Ainsworth SK, Karnovsky MJ: An ultrastructural staining method for enhancing the size and electron opacity of ferritin in thin sections. *J Histochem Cytochem* 20: 225–229, 1972